Saturation of the magnetorotational instability

Cite as: Phys. Fluids **17**, 094106 (2005); https://doi.org/10.1063/1.2047592
Submitted: 18 April 2005 • Accepted: 26 July 2005 • Published Online: 21 September 2005

Edgar Knobloch and Keith Julien

Saturation of the magnetorotational instability

Edgar Knobloch
Department of Physics, University of California, Berkeley, California 94720
and Department of Applied Mathematics, University of Leeds, Leeds LS2 9JT, United Kingdom

Keith Julien
Department of Applied Mathematics, University of Colorado, Boulder, Colorado 80309

(Received 18 April 2005; accepted 26 July 2005; published online 21 September 2005)

An analytical theory is developed that describes asymptotically exactly the process of nonlinear saturation of the magnetorotational instability in a model problem employing a linear shear flow in a uniformly rotating channel. The theory shows that the instability saturates by modifying the shear responsible for it. The saturation process requires both viscous and Ohmic dissipation. The theory also describes the approach from small-amplitude perturbations to the final strongly nonlinear saturated state. © *2005 American Institute of Physics*. [DOI: 10.1063/1.2047592]

I. INTRODUCTION

Accretion is a process of fundamental importance in astrophysics. However, accretion can only occur in the presence of an efficient mechanism for angular momentum extraction. Over the years many processes have been suggested that might lead to efficient accretion, but the current consensus is that a classical instability,[1,2] since called the magnetorotational instability (or MRI, for short), is particularly effective in this respect.[3] This instability relies on the presence of a weak poloidal field and occurs in hot disks whenever the angular velocity Ω in the disk decreases outward ($d\Omega/dr<0$). The instability grows by extracting energy from the resulting shear. Particularly noteworthy is the fact that the instability occurs on a dynamic time scale, $\tau_{\mathrm{MRI}}\sim\Omega^{-1}$, and that it is fundamentally axisymmetric. The instability has a small wavelength in the direction parallel to the rotation and magnetic field, and takes the form of thin sheets of matter moving alternately radially inward and outward. It is known that sufficient dissipation stabilizes this instability,[4] but in accretion disks dissipative processes are weak and the instability is unhindered by such processes.[3,5] It is not true, however, that dissipation is always negligible. Indeed, as shown in the present paper, for the saturation of the instability, small dissipation, both viscous and Ohmic, is required.

Because of its importance in the accretion disk problem attempts are currently underway to study this instability in the laboratory, both in the Taylor–Couette geometry where it was first discovered[2,6–9] and in a differentially rotating sphere where it has already been observed.[10] In accretion disks the MRI is believed to saturate by generating turbulence, which in turn enhances turbulent dissipation, thereby quenching the instability back to threshold. This is because the background shear is maintained by the gravitational field of the central object, and the amplitude of the turbulence is believed to remain sufficiently small that the background shear remains unperturbed, even in the fully turbulent state. In a laboratory experiment, however, the boundaries can support the radial pressure gradients that accompany any substantial modification of the shear profile. In other words, in a laboratory setting, the MRI has a different mode of saturation available to it: it can saturate by modifying the background shear that feeds it. This is the regime we explore in this paper.

The method used in the present paper has its origins in the work of Ref. 11 on the theory of Görtler vortices and related problems. Subsequently it has been used with considerable effect to study rapidly rotating convection in both two[12–14] and three dimensions,[15,16] as well as convection in a strong magnetic field.[17–19] The method takes advantage of the small scale of the instability that is used as an expansion parameter. The method is thus ideally suited for fingering instabilities such as the MRI. In the following we show that it can be applied in a straightforward fashion to the MRI in the regime of interest in which rotation and shear dominate the effects of the (poloidal) magnetic field, which is in turn more important than viscous and Ohmic dissipation. Despite this, both dissipative processes determine the final equilibrium state.

II. FORMULATION OF A MODEL PROBLEM

We consider a straight channel, $-L^*/2\leqslant x^*\leqslant L^*/2$, $-\infty<y^*<\infty$, $-\infty<z^*<\infty$, filled with an electrically conducting incompressible fluid, and rotating about the z axis with constant angular velocity Ω^*, the superscript * indicating dimensional quantities. We suppose that a linear shear flow, $\mathbf{U}_0^*=(0,\sigma^* x^*,0)$, $\sigma^*<0$, is maintained in the channel, for example, by boundaries that slide in the y direction with speeds $\pm\sigma^* L^*/2$. In addition, we suppose that a constant magnetic field, $\mathbf{B}_0^*=(0,B_{\mathrm{tor}}^*,B_{\mathrm{pol}}^*)$ is present, and consider y-independent perturbations of this state. These can be written in the form $\mathbf{u}\equiv(u,v,w)=(-\psi_z,v,\psi_x)$, $\mathbf{b}\equiv(a,b,c)=(-\phi_z,b,\phi_x)$, and satisfy the dimensionless equations

$$\nabla^2\psi_t+2\Omega v_z+J(\psi,\nabla^2\psi)=v_A^2\nabla^2\phi_z+v_A^2J(\phi,\nabla^2\phi)+\nu\nabla^4\psi, \tag{1}$$

$$v_t-(2\Omega+\sigma)\psi_z+J(\psi,v)=v_A^2 b_z+v_A^2J(\phi,b)+\nu\nabla^2 v, \tag{2}$$

$$\phi_t + J(\psi,\phi) = \psi_z + \eta\nabla^2\phi, \tag{3}$$

$$b_t + J(\psi,b) = v_z - \sigma\phi_z + J(\phi,v) + \eta\nabla^2 b, \tag{4}$$

where $v_A \equiv B^*_{\rm pol}/\sqrt{\mu_0\rho^*}U^*$ is proportional to the Alfvén speed v_A^* associated with the poloidal or vertical magnetic field, $J(f,g)\equiv f_x g_z - f_z g_x$, and Ω, ν, η represent the *dimensionless* rotation rate, kinematic viscosity, and Ohmic diffusivity, nondimensionalized using a velocity scale U^* and the channel width L^*. Note that $B^*_{\rm tor}$ drops out of these equations. This is not so in an annulus, where hoop stresses are present, and the MRI becomes oscillatory.[20,21]

In the following we assume that the MRI takes the form of thin fingers propagating in the x direction, as indicated by linear stability theory[5] and subsequent numerical experiments.[22,23] By definition, such fingers have a small transverse width. Accordingly we introduce a small parameter, $\epsilon \ll 1$, and suppose that all derivatives in the z direction are large, i.e., we scale z such that in the new variable ∂_z is replaced by $\epsilon^{-1}\partial_z$. In addition, we suppose that in an appropriate dimensionless sense the dissipative processes are weak, and let $(\nu,\eta)=\epsilon(\hat\nu,\hat\eta)$. At the same time we assume that the system is rotating rapidly and that the dimensionless shear rate is also large, i.e., we set $(\Omega,\sigma)=\epsilon^{-1}(\hat\Omega,\hat\sigma)$ while keeping the Alfvén speed of order unity. These assumptions reflect the conditions generally believed to be present in accretion disks: the shear is the dominant source of energy for the instability, but the instability itself requires the presence of a (weaker) vertical magnetic field. Dissipative effects are weaker still but cannot be ignored since they are ultimately responsible for the saturation of the instability.

It is important to specify the meaning of the small parameter ϵ. To do so we select the velocity scale U^* by the requirement that $v_A=1$. Thus $\eta=S^{-1}$, where $S \equiv B^*_{\rm pol}L^*/\eta^*\sqrt{\mu_0\rho^*}$ is the Lundquist number, and $\nu=\mathrm{Pm}\,S^{-1}$, where $\mathrm{Pm}=\nu^*/\eta^*$ is the magnetic Prandtl number. Likewise $\sigma=\mathrm{Rm}\,S^{-1}$, where $\mathrm{Rm}=|\sigma^*|L^{*2}/\eta^*$ is the magnetic Reynolds number, and $\Omega=(\Omega^*/|\sigma^*|)\mathrm{Rm}\,S^{-1}$. It follows that $\Omega\gg 1$ requires $\Omega^*L^*\gg v_A^*$ while $|\sigma|\gg 1$ requires $|\sigma^*|L^*\gg v_A^*$. In addition, the requirements $\eta\ll 1$, $\nu\ll 1$ are equivalent to $\eta^*\ll v_A^*L^*$, $\nu^*\ll v_A^*L^*$. These conditions require that $\mathrm{Rm}\gg S\gg\max(1,\mathrm{Pm})$. In our scaling these inequalities are related by the requirement that the Elsasser number $\Lambda\equiv v_A^{*2}/\Omega^*\eta^*=O(1)$, this being a regime of particular interest.[24]

In parallel with the above assumptions, we need to make further assumptions about the relative magnitude of the various fields. We find that the assumption $(\psi,\phi)\to\epsilon(\psi,\phi)$, $(v,b)\to\epsilon^{-1}(v,b)$ leads to a self-consistent fully nonlinear stationary solution, satisfying the scaled equations

$$\begin{aligned}2\epsilon^{-3}\hat\Omega v_z + \epsilon J[\psi,(\partial_x^2+\epsilon^{-2}\partial_z^2)\psi] &= v_A^2(\partial_x^2+\epsilon^{-2}\partial_z^2)\phi_z + \epsilon v_A^2 J[\phi,(\partial_x^2+\epsilon^{-2}\partial_z^2)\phi]\\ &\quad + \epsilon^2\hat\nu(\partial_x^2+\epsilon^{-2}\partial_z^2)^2\psi,\end{aligned} \tag{5}$$

$$\begin{aligned}-\epsilon^{-1}(2\hat\Omega+\hat\sigma)\psi_z + \epsilon^{-1}J(\psi,v) &= \epsilon^{-2}v_A^2 b_z + \epsilon^{-1}v_A^2 J(\phi,b) + \hat\nu(\partial_x^2+\epsilon^{-2}\partial_z^2)v,\end{aligned} \tag{6}$$

$$\epsilon J(\psi,\phi) = \psi_z + \epsilon^2\hat\eta(\partial_x^2+\epsilon^{-2}\partial_z^2)\phi, \tag{7}$$

$$\epsilon^{-1}J(\psi,b) = \epsilon^{-2}v_z - \epsilon^{-1}\hat\sigma\phi_z + \epsilon^{-1}J(\phi,v) + \hat\eta(\partial_x^2+\epsilon^{-2}\partial_z^2)b. \tag{8}$$

In these equations we have retained the parameter v_A in order to be able to vary the strength of the poloidal field *independently* of the other dimensionless quantities.

III. RESULTS

To solve Eqs. (5)–(8) we posit an expansion of the form $\psi(x,z)=\psi_0(x,z)+\epsilon\psi_1(x,z)+\cdots$, with similar expressions for the other four fields, and look for structures that are periodic in the z direction. From Eqs. (6) and (8) it now follows that at $O(\epsilon^{-2})$,

$$v_A^2 b_{0z} + \hat\nu v_{0zz} = 0, \quad v_{0z} + \hat\eta b_{0zz} = 0, \tag{9}$$

and hence that

$$v_0 = V(x), \quad b_0 = B(x), \tag{10}$$

while from Eq. (7) we obtain at $O(1)$

$$\psi_0 + \hat\eta\phi_{0z} = 0. \tag{11}$$

In addition, at next order, Eqs. (6) and (8) imply

$$-(2\hat\Omega+\hat\sigma)\psi_{0z} + J(\psi_0,v_0) = v_A^2 b_{1z} + v_A^2 J(\phi_0,b_0) + \hat\nu v_{1zz}, \tag{12}$$

$$J(\psi_0,b_0) = v_{1z} - \hat\sigma\phi_{0z} + J(\phi_0,v_0) + \hat\eta b_{1zz}. \tag{13}$$

In the following we write

$$\psi_0 = \tfrac{1}{2}[\Psi(x)e^{inz} + \text{c.c.}], \quad v_1 = \tfrac{1}{2}[\mathcal{V}(x)e^{inz} + \text{c.c.}],$$

$$\phi_0 = \tfrac{1}{2}[\mathcal{F}(x)e^{inz} + \text{c.c.}], \quad b_1 = \tfrac{1}{2}[\mathcal{B}(x)e^{inz} + \text{c.c.}]. \tag{14}$$

From Eqs. (11)–(13) it now follows that

$$\mathcal{F} = \frac{i\Psi}{\hat\eta n}, \tag{15}$$

$$\mathcal{V} = \frac{(v_A^2+\hat\eta^2 n^2)V' + \hat\eta^2 n^2(2\hat\Omega+\hat\sigma) + v_A^2\hat\sigma}{n\hat\eta(v_A^2+\hat\nu\hat\eta n^2)}i\Psi, \tag{16}$$

$$\mathcal{B} = \frac{i(v_A^2+\hat\nu\hat\eta n^2)B' + n[\hat\nu(\hat\sigma+V') - \hat\eta(2\hat\Omega+\hat\sigma+V')]}{n\hat\eta(v_A^2+\hat\nu\hat\eta n^2)}\Psi. \tag{17}$$

Finally, Eqs. (6) and (8) yield at $O(1)$ the results

$$\begin{aligned}-(2\hat\Omega+\hat\sigma)\psi_{1z} + J(\psi_0,v_1) + J(\psi_1,v_0) &= v_A^2 b_{2z} + v_A^2 J(\phi_0,b_1) + v_A^2 J(\phi_1,b_0) + \hat\nu(v_{0xx}+v_{2zz})\end{aligned} \tag{18}$$

and

$$\begin{aligned}J(\psi_0,b_1) + J(\psi_1,b_0) = v_{2z} - \hat\sigma\phi_{1z} + J(\phi_0,v_1) + J(\phi_1,v_0)\\ + \hat\eta(b_{0xx}+b_{2zz}).\end{aligned} \tag{19}$$

Averaging these equations over z and using the fact that the quantities $\psi_0,\psi_1,v_1,v_2,\phi_0,\phi_1,b_1,b_2$ are all, by construction,

periodic in z with zero mean yields the following pair of equations:

$$\hat{\nu}V'' = \partial_x(\overline{\psi_0 v_{1z}}) - v_A^2 \partial_x(\overline{\phi_0 b_{1z}}), \tag{20}$$

$$\hat{\eta}B'' = \partial_x(\overline{\psi_0 b_{1z}}) - \partial_x(\overline{\phi_0 v_{1z}}). \tag{21}$$

Thus, in the bulk, away from the boundaries at $x=\pm 1/2$, V' and B' satisfy

$$\hat{\nu}V' = \overline{\psi_0 v_{1z}} - v_A^2 \overline{\phi_0 b_{1z}}, \tag{22}$$

$$\hat{\eta}B' = \overline{\psi_0 b_{1z}} - \overline{\phi_0 v_{1z}} + C, \tag{23}$$

where the constant C is determined by force balance across the channel in the saturated state (see later). Evaluating the averages in terms of Ψ and solving for V' and B' now yields

$$V'(x) = -\frac{\frac{1}{2}\beta|\Psi|^2}{\hat{\nu} + \frac{1}{2}\alpha|\Psi|^2}, \tag{24}$$

$$B'(x) = \frac{\hat{\eta}C}{\hat{\eta}^2 + \frac{1}{2}|\Psi|^2}, \tag{25}$$

where

$$\alpha = \frac{\hat{\nu}v_A^2 + \hat{\eta}^3 n^2}{\hat{\eta}^2(v_A^2 + \hat{\nu}\hat{\eta}n^2)}, \tag{26}$$

$$\beta = \frac{(2\hat{\Omega} + \hat{\sigma})\hat{\eta}^3 n^2 + v_A^2(\hat{\sigma}\hat{\nu} - 2\hat{\Omega}\hat{\eta})}{\hat{\eta}^2(v_A^2 + \hat{\nu}\hat{\eta}n^2)}. \tag{27}$$

Equation (24) determines the equilibrated shear V' in terms of the streamfunction amplitude $|\Psi|$ and wave number n of the instability. The result does not depend on the choice of C.

We can obtain an additional relation between $|\Psi|$ and n from Eq. (5). This equation yields, at leading order,

$$2\hat{\Omega}v_{1z} = v_A^2 \phi_{0zzz} + \hat{\nu}\psi_{0zzzz}, \tag{28}$$

or, equivalently,

$$2\hat{\Omega}[(v_A^2 + \hat{\eta}^2 n^2)V' + (2\hat{\Omega} + \hat{\sigma})\hat{\eta}^2 n^2 + \hat{\sigma}v_A^2] + n^2(v_A^2 + \hat{\nu}\hat{\eta}n^2)^2 = 0. \tag{29}$$

In the following we refer to this equation as the *nonlinear* dispersion relation. This relation has an important physical interpretation: it demonstrates that in our asymptotic regime the MRI is quenched to zero growth rate by the change in the shear rate that it produces.

The relation (29) determines, for each wave number n, the equilibrium shear V' and through Eq. (24) the corresponding streamfunction amplitude Ψ. One finds

$$\frac{1}{2}|\Psi|^2[4\hat{\Omega}^2 v_A^2 \hat{\eta} + n^2(v_A^2 + \hat{\nu}\hat{\eta}n^2)(\hat{\nu}v_A^2 + \hat{\eta}^3 n^2)] + \hat{\nu}\hat{\eta}^2 n^2(v_A^2 + \hat{\nu}\hat{\eta}n^2)^2 + 2\hat{\Omega}\hat{\sigma}\hat{\nu}\hat{\eta}^2 v_A^2 + 2\hat{\Omega}(2\hat{\Omega} + \hat{\sigma})\hat{\nu}\hat{\eta}^4 n^2 = 0. \tag{30}$$

Thus Ψ, V', and B' are all *independent* of the radial coordinate x. The resulting solution thus describes the saturated state in the bulk, outside of any boundary layers introduced by boundary conditions in the transverse direction, much as occurs in linear theory.[6,8]

Equation (30) determines the amplitude $|\Psi|$ as a function of the imposed shear rate $\hat{\sigma} < 0$ for each choice of wave number n, and therefore represents the *bifurcation equation* for this problem. This relation has one particularly interesting limit: if we suppose that the $O(1)$ quantities $\hat{\Omega}$, v_A, $\hat{\eta}$, $\hat{\nu}$ in fact satisfy $\hat{\Omega} \gg v_A \gg \hat{\eta}, \hat{\nu}$, Eq. (30) reduces to

$$|\Psi|^2 = -\frac{\hat{\sigma}}{\hat{\Omega}}\hat{\nu}\hat{\eta}, \tag{31}$$

providing a simple relation between the imposed shear rate $\hat{\sigma}$ and the resulting equilibrated amplitude $|\Psi|$, and one that is *independent* of the (scaled) wave number n. Thus the (unscaled) transverse speed of the MRI fingers is of order one and is given by

$$u \sim n|\Psi| = n\left(-\frac{\hat{\sigma}}{\hat{\Omega}}\right)^{1/2}(\hat{\nu}\hat{\eta})^{1/2}, \tag{32}$$

i.e., $u^* \sim v_A^* n^* L^* S^{-1}(-\mathrm{Pm}\,\sigma^*/\Omega^*)^{1/2}$. Note that this speed is the geometric mean between the energy-containing shear flow $\sigma^* L^*$ and the dissipative scale velocities ν^*/L^* or η^*/L^*, and is accompanied by much slower $O(\epsilon)$ motions in the vertical. More significantly, Eq. (24) shows that the corresponding equilibrated shear $V' = -\hat{\sigma}$! It follows that in this limit the MRI continues until it extracts all the energy from the imposed shear and uniform rotation results. Similar behavior was observed in Ref. 22 in their original simulations of the MRI. These authors also point to the important role played by reconnection in providing a saturation mechanism, a process that appears explicitly, via the diffusivity $\hat{\eta}$, in the prediction (32).

The theory thus far remains unsatisfactory in one respect: the wave number n is not specified. It is usual in these circumstances to use the wave number, $n_{\max}$, of the fastest growing mode. According to linear theory the growth rate λ is given by

$$2\hat{\Omega}[(2\hat{\Omega} + \hat{\sigma})(\lambda + \hat{\eta}n^2)^2 + \hat{\sigma}v_A^2 n^2] + [(\lambda + \hat{\nu}n^2)(\lambda + \hat{\eta}n^2) + v_A^2 n^2]^2 = 0, \tag{33}$$

and $n_{\max}$ is defined by $d\lambda/dn = 0$. In Figs. 1–3 we show the result of using this wave number to compute the saturated state shear $V'_{\max}$ and the associated streamfunction amplitude $|\Psi|_{\max}$. The figures are computed for $\hat{\sigma} = -1.5, -1.0, -0.5$; the value -1.5 corresponds to Kepler shear. Figure 1 shows the fastest growing wave number, $n_{\max}$, the corresponding growth rate $\lambda_{\max}$, and the resulting saturated quantities $V'_{\max}$ and $|\Psi|_{\max}$ as a function of the Ohmic diffusivity $\hat{\eta}$, while Figs. 2 and 3 show these quantities as a function of v_A and $-\hat{\sigma}$, respectively. In all cases $V'_{\max}$ reaches an order one value already at very small values of $\hat{\eta}$ and then decreases toward its asymptotic value as $\hat{\eta}$ increases further. In contrast, $|\Psi|_{\max}$ increases monotonically with $\hat{\eta}$. This is as expected: resistivity permits the instability to grow to larger amplitude by allowing the magnetic field to slip through the fluid. Figure 2 shows the corresponding results as a function of v_A even though the theory permits us to set $v_A = 1$. These plots enable

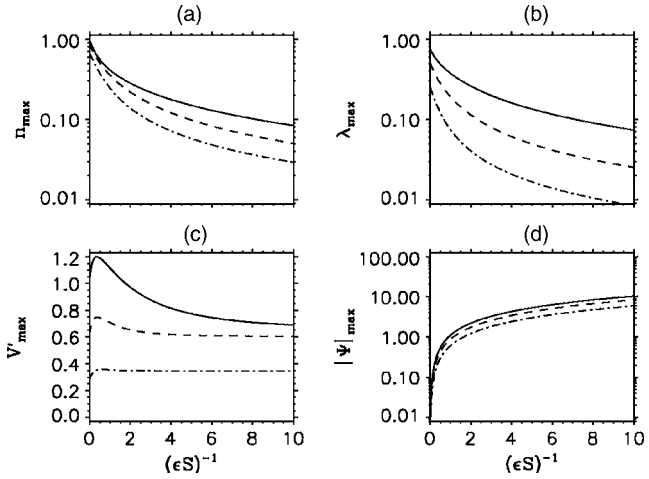

FIG. 1. (a) The wave number n_{max} of the fastest growing mode, (b) its growth rate λ_{max}, (c) the resulting shear rate V'_{max}, and (d) streamfunction amplitude $|\Psi|_{max}$, as functions of $\hat{\eta} \equiv (\epsilon S)^{-1}$ for $\hat{\Omega}=1$, $v_A=1$, $\hat{\nu}=\hat{\eta}$, and $\hat{\sigma}=-1.5,-1.0,-0.5$ (solid, dashed, dash-dotted).

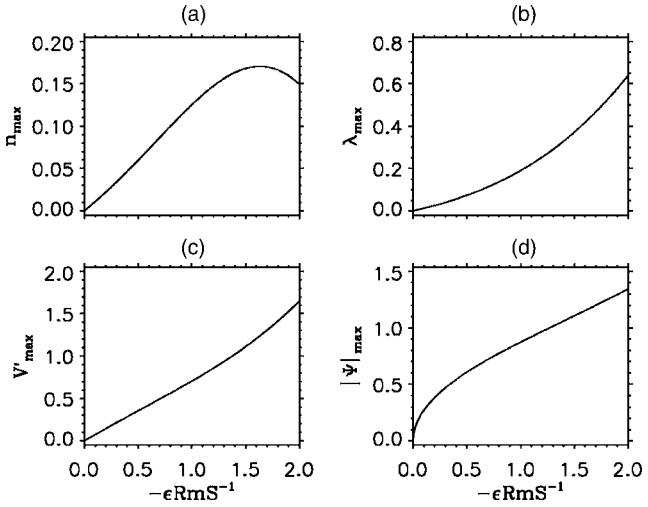

FIG. 3. The same as Fig. 1 but as functions of the ambient shear rate $\hat{\sigma} \equiv \epsilon \mathrm{Rm}\, S^{-1}$ for $\hat{\Omega}=1$, $v_A=1$, $\hat{\eta}=1$, and $\hat{\nu}=1$.

us to ascertain the role of the poloidal field for fixed values of the remaining dimensionless quantities; all results for $v_A \neq 1$ collapse onto those for $v_A=1$, provided all other parameters are adjusted to reflect the change in the Alfvén speed. The figure shows that the saturated value of V'_{max} is substantial, even for $0<v_A \ll 1$, and that this value reaches a maximum at $v_A \sim 1$ before falling slightly to its saturated value at $v_A \gg 1$. For $|\hat{\sigma}| \gtrsim 1.0$ this value exceeds that at $v_A \ll 1$, although for $|\hat{\sigma}| \lesssim 1.0$ this is no longer the case. Evidently a strong poloidal field does *not* suppress the instability in the regime of interest ($\mathrm{Rm} \gg S \gg 1$), an observation consistent with the linear theory results.[8] Together these figures indicate that both V'_{max} and $|\Psi|_{max}$ increase with the background shear $|\hat{\sigma}|$, the former rather more dramatically than the latter. Figure 3 shows that this increase is monotonic and approximately linear. Finally, Fig. 4 shows that the (scaled) vertical wave number n predicted by the nonlinear dispersion relation (29) vanishes when $V'=-\hat{\sigma}$, indicating an increase in the vertical wavelength as the MRI approaches saturation.

It remains to interpret the constant C in Eq. (25). For this purpose we take an average over z of the dimensionless transverse balance relation

$$\mathbf{u} \cdot \nabla u - 2\Omega v = -p_x + v_A^2 \left((\mathbf{B}_0 + \mathbf{b}) \cdot \nabla a - \frac{1}{2} |\mathbf{B}_0 + \mathbf{b}|_x^2 \right). \tag{34}$$

In the scaled variables the resulting leading-order balance takes the form

$$\hat{p}_{0x} = (2\hat{\Omega} V' - v_A^2 B'^2) x, \tag{35}$$

where $\hat{p}_0$ is a suitably scaled pressure contribution. Thus $C=0$ if the shear is supported entirely by a mechanical pressure gradient, $0<C<C_{max}$ if it is partly supported by a magnetic pressure gradient, while $C=C_{max}$ when $2\hat{\Omega} V' = v_A^2 B'^2$, i.e.,

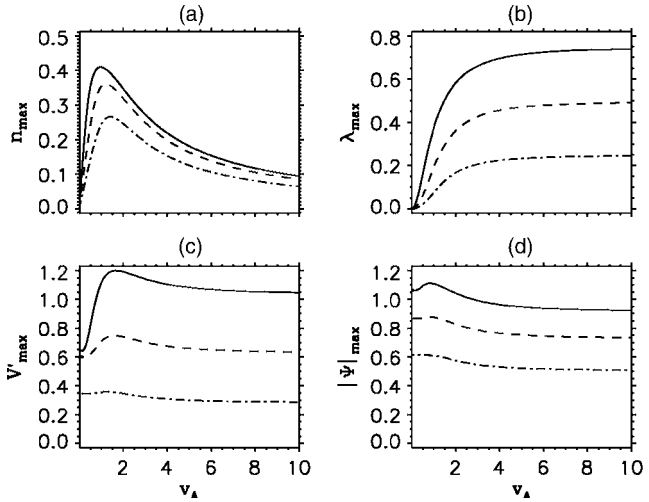

FIG. 2. The same as Fig. 1 but as functions of v_A for $\hat{\Omega}=1$, $\hat{\eta}=1$, $\hat{\nu}=1$, and $\hat{\sigma}=-1.5,-1.0,-0.5$. The instability is absent when $v_A \equiv 0$.

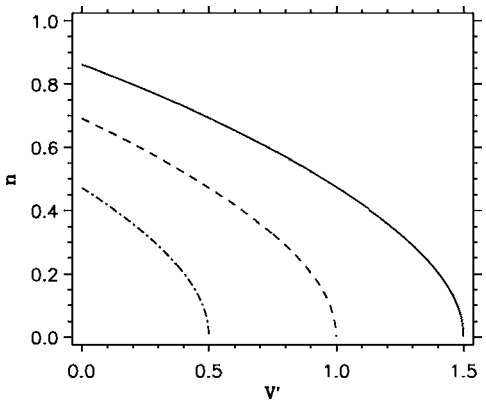

FIG. 4. The vertical wave number n computed from the nonlinear dispersion relation (29) as a function of V' for $\hat{\Omega}=1$, $v_A=1$, $\hat{\nu}=\hat{\eta}=1$, and $\hat{\sigma}=-1.5$, $-1.0,-0.5$ (solid, dashed, dash-dotted).

$$C_{\max}^2 = -\frac{\hat{\Omega}\beta}{v_A^2\hat{\eta}^2}\frac{\left(\hat{\nu}^2+\frac{1}{2}|\Psi|^2\right)^2}{\hat{\nu}+\frac{1}{2}\alpha|\Psi|^2}|\Psi|^2. \tag{36}$$

The results presented below span the range $0 \leqslant C \leqslant C_{\max}$.

IV. APPROACH TO THE SATURATED STATE

It is of interest to examine the approach from an initial small-amplitude state with $V' \sim 0$ to the final equilibrated state (24). To do this we note that the MRI evolves initially on a dynamical or rotation time scale, i.e., the fast time $\tau \equiv t/\epsilon = O(1)$. However, examining the structure of the equations in the long time limit, we also notice that the final approach to the saturated state proceeds on the much slower time scale $T \equiv \epsilon t = O(1)$, i.e., on the resistive time scale. These observations suggest a multiple time scale expansion. It is simpler, however, to assume formally that after a brief $[\tau = O(1)]$ transient both V' and B' evolve on a slower time scale than the remaining fields, and take V' and B' to be independent of x. In this regime, ψ_0, v_1, ϕ_0, and b_1 are functions of z and τ only, and satisfy

$$v_{1\tau} - (2\hat{\Omega} + \hat{\sigma} + V')\psi_{0z} = v_A^2 b_{1z} - v_A^2 B' \phi_{0z} + \hat{\nu} v_{1zz}, \tag{37}$$

$$\phi_{0\tau} = \psi_{0z} + \hat{\eta}\phi_{0zz}, \tag{38}$$

$$b_{1\tau} - \psi_{0z}B' = v_{1z} - (\hat{\sigma} + V')\phi_{0z} + \hat{\eta} b_{1zz}, \tag{39}$$

together with

$$\psi_{0zz\tau} + 2\hat{\Omega} v_{1z} = v_A^2 \phi_{0zzz} + \hat{\nu}\psi_{0zzzz}. \tag{40}$$

These equations are separable in z and τ. Assuming the ansatz (14), we obtain

$$\mathcal{V}_\tau + \hat{\nu} n^2 \mathcal{V} = in(2\hat{\Omega} + \hat{\sigma} + V')\Psi + inv_A^2 \mathcal{B} - inv_A^2 B' \mathcal{F}, \tag{41}$$

$$\mathcal{F}_\tau + \hat{\eta} n^2 \mathcal{F} = in\Psi, \tag{42}$$

$$\mathcal{B}_\tau + \hat{\eta} n^2 \mathcal{B} = in\Psi B' + in\mathcal{V} - in(\hat{\sigma} + V')\mathcal{F}, \tag{43}$$

$$\Psi_\tau + \hat{\nu} n^2 \Psi - 2in^{-1}\hat{\Omega}\mathcal{V} - inv_A^2 \mathcal{F} = 0. \tag{44}$$

Here V' and B' are functions of τ only, and are given by

$$\hat{\nu} V' = -\tfrac{1}{4} in(\Psi \mathcal{V}^* - \Psi^* \mathcal{V}) + \tfrac{1}{4} inv_A^2 (\mathcal{F}\mathcal{B}^* - \mathcal{F}^* \mathcal{B}), \tag{45}$$

$$\hat{\eta} B' = -\tfrac{1}{4} in(\Psi \mathcal{B}^* - \Psi^* \mathcal{B}) + \tfrac{1}{4} in(\mathcal{F}\mathcal{V}^* - \mathcal{F}^* \mathcal{V}) + C. \tag{46}$$

These equations capture correctly the saturation process, and, in particular, the final steady state. The resulting evolution of $V'(\tau)$ and the associated toroidal field gradient $B'(\tau)$ are shown in Fig. 5(a) starting from small-amplitude initial conditions. The evolution is shown over times $\tau = O(\epsilon^{-2})$ and shows unambiguously the convergence of V' toward its saturated value (24), regardless of C; the latter determines B' only [Eq. (25)]. For comparison we also show the evolution of the amplitude $|\Psi|$ of the streamfunction [Fig. 5(b)].

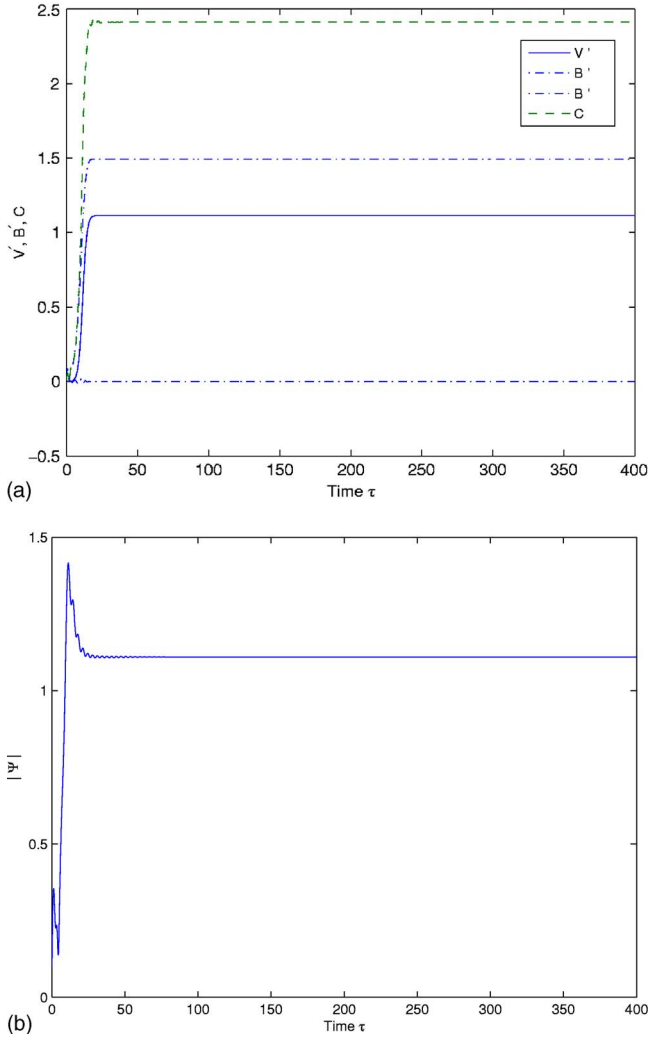

FIG. 5. (a) The approach of the MRI to its saturated state, computed for $\hat{\Omega}=1$, $\hat{\sigma}=-1.5$, $v_A=1$, $\hat{\eta}=1$, $\hat{\nu}=1$, showing the evolution of V' (solid line) and B' (dashed-dotted lines) from small-amplitude initial conditions when $C=0$ and $C=C_{\max}$ (dashed line). For these parameter values the equilibrated value $V'=-0.71\hat{\sigma}$. (b) The corresponding evolution of $|\Psi|$.

V. DISCUSSION

In this paper we have shown that a simple scaling suffices to determine and fully characterize a self-consistent equilibrated state of the magnetorotational instability in a rotating horizontal channel. This state is associated with a substantial modification of the background shear that feeds the instability, and is ultimately determined by both viscous and Ohmic dissipation. In our picture this state is reached after an $O(\Omega^{-1})$ transient followed by a slower evolution on a time scale v_A^{-1}, although the final stages of saturation occur on the much slower time scale η^{-1}, ν^{-1} associated primarily with reconnection. The theory, in fact, identified a one-parameter family of steady states, parametrized by the parameter C in Eq. (25) that measures the contribution of the longitudinal (toroidal) magnetic field to the force balance in the transverse direction. However, the associated modification of the background shear is independent of C and is constant in the bulk, outside of thin boundary layers at $x = \pm 1/2$ required by the sliding boundary conditions. These

boundary layers are evident in linear theory, but do not affect the structure of the unstable modes in the bulk.[6,8] In other problems of this type (e.g., Refs. 12 and 13), the nonlinear dispersion relation (29) is replaced by a nonlinear *eigenvalue* problem for $\Psi(x)$ and the associated shear profile, and the boundary layer structure is then considerably different. It should be noted that in the theory the equilibrated state in the bulk consists of laminar axisymmetric "fingers" and is not a turbulent state such as might result from shear instabilities between neighboring fingers.[25] In some cases, however, the resulting turbulent state may reflect in its statistical properties the presence of the underlying laminar state,[15,26] while in others this laminar state *overestimates* the transport properties of the turbulence.

It is of interest to compare our results with the original simulation of the instability by Hawley and Balbus that employed reflecting boundary conditions in the radial direction.[22] Although unable to reach the saturated state the simulations revealed a clear tendency toward solid body rotation as the instability grew. The authors also argued that the saturated speed of the fingers should be of order v_A, as predicted by Eq. (32). However, the prediction (32) shows that while the order of magnitude is correct the saturated speed is not proportional to v_A. Indeed, it is independent of the vertical magnetic field entirely, as might be expected of an instability whose onset is independent of B_z together with a saturation process that relies on efficient reconnection. Subsequent simulations using the shearing sheet approximation reveal a tendency toward increasing wavelength as the instability proceeds,[23] an observation that is consistent with the predictions of Eq. (29). It is likewise relevant that two-dimensional shearing sheet simulations of the MRI with resistivity but no viscosity[24] show saturation for $\Lambda \lesssim 1$ but not for $\Lambda \gtrsim 1$. This lack of saturation is typical of situations where the instability is not permitted to modify the background shear.[25] In contrast, the theory described here shows that if such a modification is permitted saturation does in fact occur in both regimes, provided only that both Ohmic dissipation *and* viscosity are included in the theory.

The theory described here applies formally to the small gap limit of the Taylor–Couette system, in which the shear flow profile can be approximated by a linear profile. In such a system $\hat{\sigma}=-1$, and the modified shear profile produced in the bulk by the growing MRI can be balanced by an appropriate radial pressure gradient. Thus, the constant C in the theory can be set to zero. Moreover, we believe that the insight gained from the theory has value beyond the Taylor–Couette system, and may well apply to existing experiments on the MRI in differentially rotating spheres.[10] We hope, likewise, that the analytical progress made here in identifying the mechanisms leading to saturation of the instability and characterizing the final stationary state may encourage new theoretical studies of this important instability. For example, the stability properties of the saturated state with respect to three-dimensional perturbations may shed additional light on the saturation process. An extension of the theory to circular geometry, and, in particular, to larger gap annuli, will be presented elsewhere.

ACKNOWLEDGMENTS

This work was carried out while the first author (E.K.) was a participant in a 2004 Newton Institute programme on Magnetohydrodynamics of Stellar Interiors in Cambridge, UK. The second author (K.J.) acknowledges financial support from a University of Colorado Faculty Fellowship Award. Both are grateful to E. Kersalé and S. Tobias for helpful comments.

[1] E. P. Velikhov, "Stability of an ideally conducting liquid flowing between cylinders rotating in a magnetic field," Sov. Phys. JETP **36**, 995 (1959).
[2] S. Chandrasekhar, "The stability of non-dissipative Couette flow in hydromagnetics," Proc. Natl. Acad. Sci. U.S.A. **46**, 253 (1960).
[3] S. A. Balbus and J. F. Hawley, "Instability, turbulence, and enhanced transport in accretion disks," Rev. Mod. Phys. **70**, 1 (1998).
[4] D. Acheson and R. Hide, "Hydromagnetics of rotating fluids," Rep. Prog. Phys. **36**, 159 (1973).
[5] S. A. Balbus and J. F. Hawley, "A powerful local shear instability in weakly magnetized disks. I. Linear analysis," Astrophys. J. **376**, 214 (1991).
[6] H. Ji, J. Goodman, and A. Kageyama, "Magnetorotational instability in a rotating liquid metal annulus," Mon. Not. R. Astron. Soc. **325**, L1 (2001).
[7] G. Rüdiger and Y. Zhang, "MHD instability in differentially-rotating cylindric flows," Astron. Astrophys. **378**, 302 (2001).
[8] J. Goodman and H. Ji, "Magnetorotational instability of dissipative Couette flow," J. Fluid Mech. **462**, 365 (2002).
[9] A. P. Willis and C. F. Barenghi, "Magnetic instability in a sheared azimuthal flow," Astron. Astrophys. **388**, 688 (2002).
[10] D. R. Sisan, N. Mujica, W. A. Tillotson, Y.-M. Huang, W. Dorland, A. B. Hassam, T. M. Antonsen, and D. P. Lathrop, "Experimental observation and characterization of the magnetorotational instability," Phys. Rev. Lett. **93**, 114502 (2004).
[11] P. J. Blennerhassett and A. P. Bassom, "Nonlinear high-wavenumber Bénard convection," IMA J. Appl. Math. **52**, 51 (1994).
[12] A. P. Bassom and K. Zhang, "Strongly nonlinear convection cells in a rapidly rotating fluid layer," Geophys. Astrophys. Fluid Dyn. **76**, 223 (1994).
[13] K. Julien and E. Knobloch, "Fully nonlinear oscillatory convection in a rotating layer," Phys. Fluids **9**, 1906 (1997).
[14] K. Julien and E. Knobloch, "Strongly nonlinear convection cells in a rapidly rotating fluid layer: the tilted *f*-plane," J. Fluid Mech. **360**, 141 (1998).
[15] K. Julien, E. Knobloch, and J. Werne, "A new class of equations for rotationally constrained flows," Theor. Comput. Fluid Dyn. **11**, 251 (1998).
[16] K. Julien and E. Knobloch, "Fully nonlinear three-dimensional convection in a rapidly rotating layer," Phys. Fluids **11**, 1469 (1999).
[17] P. C. Matthews, "Asymptotic solutions for nonlinear magnetoconvection," J. Fluid Mech. **387**, 397 (1999).
[18] K. Julien, E. Knobloch, and S. Tobias, "Strongly nonlinear magnetoconvection in three dimensions," Physica D **128**, 105 (1999).
[19] K. Julien, E. Knobloch, and S. Tobias, "Nonlinear magnetoconvection in the presence of strong oblique fields," J. Fluid Mech. **410**, 285 (2000).
[20] E. Knobloch, "On the stability of magnetized accretion disks," Mon. Not. R. Astron. Soc. **255**, P25 (1992).
[21] E. Knobloch, "Symmetry and instability in rotating hydrodynamic and magnetohydrodynamic flows," Phys. Fluids **8**, 1446 (1996).
[22] J. F. Hawley and S. A. Balbus, "A powerful local shear instability in weakly magnetized disks. II. Nonlinear evolution," Astrophys. J. **376**, 223 (1991).
[23] J. F. Hawley and S. A. Balbus, "A powerful local shear instability in weakly magnetized disks. III. Long-term evolution in a shearing sheet," Astrophys. J. **400**, 595 (1992).
[24] T. Sano, S. Inutsuka, and S. M. Miyama, "A saturation mechanism of magnetorotational instability due to Ohmic dissipation," Astrophys. J. Lett. **506**, L57 (1998).
[25] J. Goodman and G. Xu, "Parasitic instabilities in magnetized, differentially rotating disks," Astrophys. J. **432**, 213 (1994).
[26] G. Kawahara and S. Kida, "Periodic motion embedded in plane Couette turbulence; regeneration cycle and burst," J. Fluid Mech. **449**, 291 (2001).